Journal of Applied Fluid Mechanics, Vol. 9, No. 6, pp. 3001-3011, 2016.
Available online at www.jafmonline.net, ISSN 1735-3572, EISSN 1735-3645.
DOI: 10.29252/jafm.09.06.24903

Combination between the Inclinations of the Enclosure and the Magnetic Field Orientation on the Oscillatory Natural Convection

A. Atia[1], S. Bouabdallah[1,2†] and B. Ghernaout[1]

[1] *Laboratory of Mechanics, University of Laghouat, Laghouat 03000, Algeria*
[2] *LEAP, University of Constantine-1, Constantine 25000, Algeria*

†*Corresponding Author Email: fibonsaid@gmail.com*

(Received April 11, 2015; accepted May 11, 2016)

ABSTRACT

In this paper, we study the combination between the inclinations of the enclosure and the magnetic field orientation on the oscillatory natural convection. For this, a cylindrical enclosure filled with electrically conducting fluid, has an aspect ratio equal to 2, and subjected to a vertical temperature gradient and different uniform magnetic field orientations were considered. The finite volume method is used to discretize the equations of continuity, momentum and energy. Our computer program based on the SIMPLER Algorithm has a good agreement with available experimental and numerical results. The time-dependent flow and temperature field are presented in oscillatory state, for different cases: inclination of the cylinder, under the effect of magnetic field in different orientations ($\delta = 0°$, 30°, 45° and 90°) and the combination between them. The results are presented at various inclinations of the cylinder ($\varphi = 0°$, 30° and 45°), and the Hartmann numbers $Ha \leq 50$. The stability diagrams of the dependence between the complicated situations with the value of the critical Grashof number Gr_{cr} and corresponding frequency Fr_{cr}, are established according to the numerical results of this investigation. The combination between the studied state has a significant effect on the stabilization of the convective flow, and shows that the best stabilization of oscillatory natural convection is obtained at the inclination of the cylinder $\varphi = 30°$, and the applied of radial magnetic field ($\delta = 0°$).

Keywords: Natural convection; Magnetic field; Oscillatory convection; Inclined cylinder.

NOMENCLATURE

Ar	aspect ratio
B	intensity of magnetic field
Br	radial magnetic field
Bz	axial magnetic field
C_p	specific heat at constant pressure of liquid
F_{EMr}	dimensionless Lorentz force in the r-direction
F_{EMz}	dimensionless Lorentz force in z-direction
Fr	dimensionless frequency pressure
g	gravitational acceleration
Gr	Grashof number
H	height of the cylinder
Ha	Hartmann number
Nu_{avg}	average Nusselt number
P	dimensionless pressure
Pr	Prandtl number
R	radius of the cylinder, m
r, z	dimensionless coordinates
T	temperature
u, v	dimensionless radial and axial velocity
α	thermal diffusivity
β	thermal expansion coefficient
δ	orientation of the magnetic field
θ	dimensionless temperature
ρ	density of the fluid
σ	electric conductivity
τ	dimensionless time
υ	kinematic viscosity
φ	inclination of cylinder
Ψ	dimensionless stream function

Subscripts

c	cold
cr	critical value
h	hot
max	maximum value

1. INTRODUCTION

In recent years, various studies dealing with natural convection in inclined enclosures have been reported. These studies show that tilting the enclosure have a significant effect on the flow and heat transfer characteristics. For instance, in crystal growth processes from melts, it has been reported by Markham *et al*. (1984) that larger transports rated are obtained by tilting the ampoule. Motivated by this, Bontoux *et al*. (1986) have carried out a numerical and experimental investigation on three-dimensional buoyancy-driven flows in a tilted cylinder (ampoule) with axial heating. Many other examples on the effect of inclination on natural convection flows have been reported by Delgado-Buscalioni and Crespo del Arco (2001). For example, it has been proved that significant heat transfer enhancement can be obtained when the tube in a heat exchanger is optimally inclined (see Lock and Fu, 1993). Other applications of inclined configurations are the honeycomb solar collector plates (Wirtz and Tsheng 1970, 1980), spread of radioactive materials in long tilted liquid-filled rock fractures (Woods and Linz, 1992) and geophysical situations where a fluid is enclosed in narrow slots arbitrarily inclined to gravity (Cessi and Young, 1992). Also, Cerisier and Rahal (1996) have employed inclined geometries in their experimental investigation on natural convection in enclosures with axial and lateral heating to study the interaction between longitudinal and transversal instabilities.

Natural convection in enclosures under the effect of magnetic fields has also received considerable attention in recent years due to possible applications in many industrial and technological fields such as fusion reactors and crystal growth. For example, Oreper and Szekely (1983) have found that the strength of the magnetic field is one of the important factors in determining the quality of the crystal. This is related to the fact that during a crystal growth process, some turbulence in the natural convection currents occurs. This can be suppressed by the application of a magnetic field. Gelfgat and Bar-Yoseph (2001) studied numerically the effect of an external magnetic field with different magnitudes and orientations in a rectangular cavity. Stability diagrams for the dependence of the critical Grashof number on the Hartmann number were obtained by the authors. They showed that a vertical magnetic field provides a strongest stabilizing effect, and also that the multiplicity of steady states is suppressed by the electromagnetic effect. Bouabdallah and Bessaïh (2012) studied the effect of a magnetic field orientation on fluid flow and heat transfer during solidification from a melt in a cubic enclosure. They have shown a strong dependence between the interface shape and the intensity and orientation of magnetic field and the strongest stabilization of the flow field and heat transfer are shown when the magnetic field is oriented vertically ($\gamma = 90°$). Similar results have also been obtained by Battira and Bessaïh (2008). Oudina and Bessaïh (2014) studied the effect of a magnetic field orientation in a cylindrical configuration filled with a low-Prandtl number electrically conducting fluid. Their study confirms the possibility of stabilization of a liquid metal flow in natural convection by application of a radial magnetic field. Ozoe and Maruo (1987) investigated numerically the natural convection of a low Prandtl number fluid in the presence of a magnetic field and obtained correlations for the Nusselt number in terms of Rayleigh, Prandtl and Hartmann numbers. Garandet *et al*. (1992) proposed an analytical solution to the governing equations of MHD to be used to model the effect of a transverse magnetic field on natural convection in a two-dimensional cavity. Seth and Ghosh (1986) proposed unsteady hydromagnetic flow in a rotating channel in the presence of an inclined magnetic field. Ghosh (1991) proposed a note on steady and unsteady hydromagnetic flow in a rotating channel in the presence of an inclined magnetic field. After, they proposed a note for unsteady hydromagnetic flow in a rotating channel permeated by an inclined magnetic field in the presence of an oscillator (Ghosh, 1997 and Ghosh and Pop, 2002). They examined also in their next work Ghosh *et al*. (2010), the transient hydromagnetic flow in a rotating channel permeated by an inclined magnetic field with magnetic induction and Maxwell displacement current effects. Rudraiah *et al*. (1995) investigated the effect of a transverse magnetic field on natural convection flow inside a rectangular enclosure with isothermal vertical walls and adiabatic horizontal walls and found out that a circulating flow is formed with a relatively weak magnetic field and that the convection is suppressed and the rate of convective heat transfer is decreased when the magnetic field strength increases. Alchaar *et al*. (1995) investigated numerically the natural convection in a shallow cavity heated from below in the presence of an inclined magnetic field and showed that the convection modes inside the cavity strongly depend on both the strength and orientation of the magnetic field and that horizontally applied magnetic field is the most effective in suppressing the convection currents. Al-Najem *et al*. (1998) used the power law control volume approach to determine the flow and temperature fields under a transverse magnetic field in a tilted square enclosure with isothermal vertical walls and adiabatic horizontal walls at Prandtl number equal 0.71, and showed that the suppression effect of the magnetic field on convection currents and heat transfer is more significant for low inclination angles and high Grashof numbers. Buhler (1995) has considered MHD flows in arbitrary geometries in strong magnetic fields related to the design of fusion reactor blankets. Viskanta *et al*. (1986) have studied three-dimensional natural convection heat transfer of a liquid metal in a cavity. Tagawa and Ozoe (Tagawa and Ozoe 1997, 1998) have reported on the enhancement of heat transfer rate by the application of a static magnetic field in a cubical enclosure. Piazza and Ciofalo (2002) have analyzed MHD free convection in a liquid-metal filled cubic enclosure for the conditions of differential heating and internal heating.

Recently, Ramana Reddy *et al*. (2016) presented the

MHD mixed convection oscillatory flow over a vertical surface in a porous medium with chemical reaction and thermal radiation. They analysed the influence of a first-order homogeneous chemical reaction, heat source and Soret effects are analyzed. They conclude that, the velocity decreases with increasing the Prandtl number, and magnetic field parameter whereas reverse trend is seen with increasing the heat generation parameter, radiation parameter, porous parameter, Soret number, thermal and solutal Grashof numbers. The temperature decreases as the values of Prandtl number increase and reverse trend is seen by increasing the values of the thermal radiation parameter, heat source parameter. The concentration decreases as the values of the chemical reaction parameter and Schmidt number whereas concentration increases with increase the value of Soret number.

To our knowledge, the combination between the magnetic field orientation and the inclinations of the cylinder enclosure on the oscillatory natural convection has never been studied, except for the case treated recently by Oudina and Bessaïh (2014), but with axial and radial magnetic field applied without inclination of the enclosure. Therefore, the objective of the present contribution is to study the combination between the inclinations of the cylinder enclosure and the magnetic field orientation on the oscillatory natural convection. The study was carried out in oscillatory state, for different cases: inclination of the cylinder (φ= 0°, 30° and 45°), under the magnetic field at different orientations (δ =0, 30°, 45° and 90°, Ha $\leq$ 50), and the combination between them. The critical Grashof number Gr_{cr} and corresponding critical frequency Fr_{cr} associated with different inclinations of cylinder φ and Hartmann numbers/different orientations δ are determined in each case and discussed. Section 2 presents the geometry and mathematical model. Section 3 discusses the numerical method and techniques, which have been used for the computation; Section 4 presents the results and discussion: computer code validation, effect of the inclination of the cylinder enclosure, effect of the magnetic field orientation and the combination between them. Finally, a conclusion is given.

2. GEOMETRY AND MATHEMATICAL MODEL

The geometry considered is a cylindrical enclosure (Fig.1) of radius R and height H, thus with an aspect ratio Ar = H/R = 2. The enclosure filled completely with a molten metal (InP), have a Prandtl number equal Pr = 0.015. The horizontal walls of the enclosure are maintained at different temperatures, the bottom wall is maintained at the hot temperature T_h while the top wall maintained at the cold temperature T_c (T_h >T_c). The side wall is supposed adiabatic. The inclination of the cavity was also considered, with a varying angle φ between the heated wall and the horizontal axis. The flow is subjected to the action of an external uniform magnetic field with different orientations. Electrically, the walls of the cylindrical enclosure are insulated. The induced magnetic field is negligible because the magnetic Reynolds number Re_m is much smaller than unity (Seth *et al*. 2012). By neglecting the dissipation and Joule heating, and using R, υ/R, R^2/υ, ρ $(\upsilon R)^2$ and (T_h-T_c) as typical scales for lengths, velocities, time, pressure and temperature, respectively. The dimensionless governing equations for the conservation of mass, momentum, and energy with the Boussinesq approximation, together with appropriate initial and boundary conditions in the cylindrical coordinates system (r, z), are written in dimensionless form, as follows:

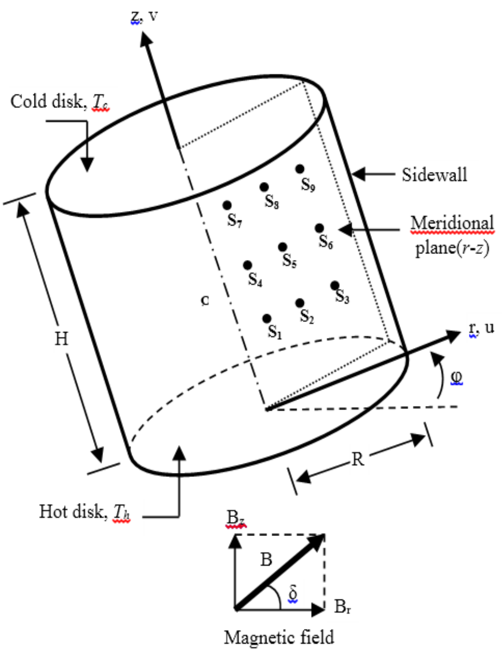

(a) Physical problem with local positions of the monitoring points: S_1, S_2, S_3, S_4, S_5, S_6, S_7, S_8 and S_9

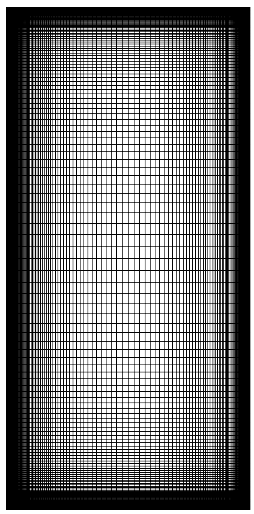

(b) Computational domain (80×160)

Fig. 1. Geometry and computational domain with boundary conditions.

Continuity equation

$$\frac{1}{r}\frac{\partial(ru)}{\partial r}+\frac{\partial v}{\partial z}=0 \quad (1)$$

R-Momentum equation

$$\frac{\partial u}{\partial t}+u\frac{\partial u}{\partial r}+v\frac{\partial u}{\partial z}=-\frac{\partial p}{\partial r}+\left[\frac{1}{r}\frac{\partial}{\partial r}\left(r\frac{\partial u}{\partial r}\right)+\frac{\partial^2 u}{\partial z^2}-\frac{u}{r^2}\right]+Gr.\theta.\sin(\varphi)+F_{EMr} \quad (2)$$

Z-Momentum equation

$$\frac{\partial v}{\partial t}+u\frac{\partial v}{\partial r}+v\frac{\partial v}{\partial z}=-\frac{\partial p}{\partial z}+\left[\frac{1}{r}\frac{\partial}{\partial r}\left(r\frac{\partial v}{\partial r}\right)+\frac{\partial^2 v}{\partial z^2}\right]+Gr.\theta.\cos(\varphi)+F_{EMz} \quad (3)$$

Energy equation

$$\frac{\partial \theta}{\partial t}+u\frac{\partial \theta}{\partial r}+v\frac{\partial \theta}{\partial z}=\frac{1}{\Pr}\left[\frac{1}{r}\frac{\partial}{\partial r}\left(r\frac{\partial \theta}{\partial r}\right)+\left(\frac{\partial^2 \theta}{\partial z^2}\right)\right] \quad (4)$$

In Eqs. (2) and (3), F_{EMr} and F_{EMz} represent the Lorentz forces components in the r and z directions respectively (Bessaïh and Bouabdallah, 2008), u and v are the dimensionless velocity components in the radial and axial directions, P is the dimensionless pressure and θ is the dimensionless temperature. So, the resulting dimensionless numbers are: Grashof number $Gr=g\beta(T_h-T_c)R^3/\upsilon^2$, Prandtl number $\Pr=\upsilon/\alpha$ and Hartmann number $Ha=Br\sqrt{\sigma/\rho\upsilon}$, which indicate the ratio of the electromagnetic forces to the viscosity forces. The quantities g, β, ρ, υ and σ are the gravity acceleration, the thermal expansion coefficient, the density, the kinematic viscosity and the electric conductivity of the fluid, respectively.

The above equations are solved subject to the following initial and boundary conditions:

The initial conditions, at τ = 0,

u = v = θ = 0 (5a)

The boundary conditions of the dimensionless quantities (u, v and θ) for τ > 0 are:

- Along the bottom wall (z = 0, 0 ≤ r ≤ 1);

u = v = 0, θ = 1 (5b)

- Along the top wall (z = Ar; 0 ≤ r ≤ 1);

u = v = 0, θ = 0 (5c)

- Along the sidewall (0 ≤ z ≤ Ar; r = 1);

$$u = v = 0,\ \frac{\partial \theta}{\partial r}=0 \quad (5d)$$

- Along the symmetry axe (0 ≤ z ≤ Ar; r = 0);

$$u = 0,\ \frac{\partial v}{\partial r}=0,\ \frac{\partial \theta}{\partial r}=0 \quad (5e)$$

3. NUMERICAL METHOD

The governing equations (Eqs. (1)-(4)) with the associated boundary and initial conditions (Eqs. 5a-e) are solved using a finite volume method. Scalar quantities are stored at the center of control volume, whereas the vectorial quantities are stored on the faces of each volume. For the discretization of spatial terms, a second-order central difference scheme is used for the diffusion and convection terms of the mathematical model, and the SIMPLER Algorithm (Patankar, 1980) is used to determine the pressure from continuity equation. The obtained algebraic equations are solved by the line-by-line tri-diagonal matrix algorithm (TDMA). The convergence is declared when the maximum relative change between two consecutive iteration levels fell below than 10^{-5}.

The increments Δr and Δz of the grid are not regular, they are chosen according to geometric progressions of ratio equal to 1.05 (Atia *et al*. 2015), which permitted grid refinement near the walls, in the Hartmann layer where large velocity and temperature gradients exist, thus requiring a larger number of nodes in order to resolve the specific characteristics of the magnetohydrodynamic flow, also in order to reduce numerical errors.

The grid independency tests are presented in Table 1 which includes the values of the stream function and the average Nusselt number for different grid sizes. We can notice that the relative error between all grids is very low, and does not exceed 7%. We also see that the low relative error occurs between the two meshes 80 × 160 and 90 × 180. It does not exceed 1% indicated that it gives the same numerical solution of the problem. So, the grid used has 80×160 nodes (the same computation domain used in the work of Oudina and Bessaïh, 2014 and Bessaïh *et al*. 2009). This grid is considered to show the best compromise between computational time and precision. Calculations were carried out on a PC with a 2.8 GHz CPU. Thus, the average computing time for a typical case was approximately 8 hours.

Table 1 Effect of grid size on the stream function and the average Nusselt number for Gr = 10^5, φ = 30°, Pr = 0.015 and Ha = 0

Grid $n_r \times n_z$	$\lvert\Psi_{max}\rvert$	Nu_{avg}
50 × 100	34.028	3.364
60 × 120	34.022	3.352
70 × 140	34.004	3.301
80 × 160	34.00	3.282
90 × 180	34.001	3.282

4. RESULTS AND DISCUSSION

4.1 Computer Code Validation

To allocate more confidence in our numerical results, we have established some comparisons with other experimental and numerical investigations available in the literature. Firstly, a comparison is presented between our numerical results and those obtained by the authors (Kakarantzas *et al*. 2009, Karcher *et al*. 2002, Mahfoud and Bessaïh, 2012). They used a cylindrical cavity of aspect ratio Ar = 4.125 (in this study Ar = R / H), filled with a fluid of low Prandtl number Pr = 0.0203 (liquid alloy GaInSn in eutectic composition), the bottom and lateral wall cooled by circulation of the water, and the upper wall heated electrically. The maximum value of the temperature versus the Hartmann number Ha is presented in Fig. 2a. A good agreement between the obtained and reported results was observed.

Secondly, the comparison has been made for the vertical distribution of the radial velocity u at r = 0.25, with experimental measurements obtained by Karcher *et al*. (2002), for Ha = 0 (Fig. 2b). It is clear that the computed values can be seen to be in excellent agreement with the measurements. These comparisons validate our computer code by assigning the desired confidence to use.

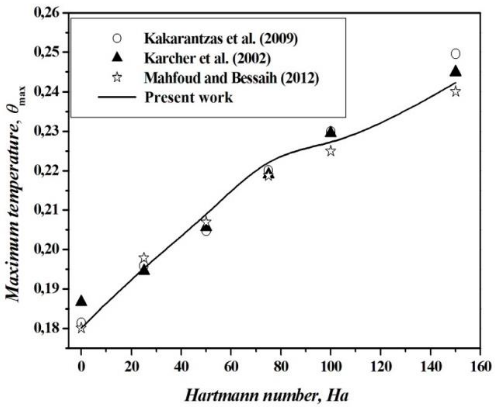

(a)

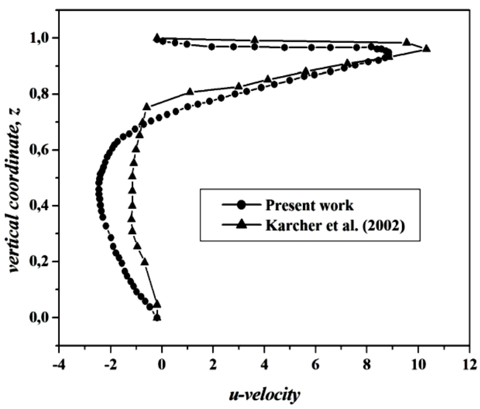

(b)

Fig. 2. Comparison between our results and previous numerical/experimental studies.

4.2 Effect of the Inclinations of the Enclosure on the Oscillatory Natural Convection (φ ≠ 0°)

We are interested herein to the flow behavior in the absence of magnetic field (Ha = 0). The Eqs. (1)-(4) are solved numerically without taking into account the Lorentz forces F_{EMr} and F_{EMz} in the Navier-Stokes equations. The calculation of the oscillatory solution consists on the determination of the critical Grashof number Gr_{cr}, for which the flow becomes oscillatory and periodic in time. The reason of these oscillatory instabilities is closely related to the mechanism of production of the secondary cells. This case is a good agreement with the results obtained by Gelfgat and Taansawa (1994), which supposed the instability is caused by the interaction between the central vortex and the smallest vortices.

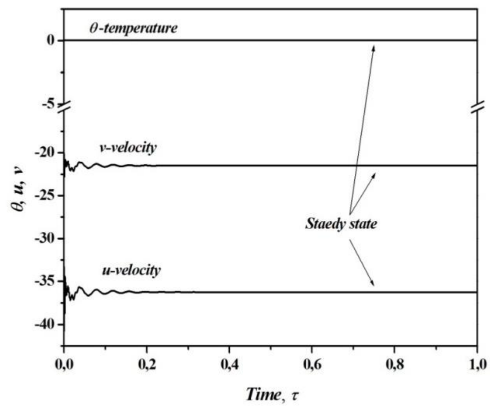

(a)

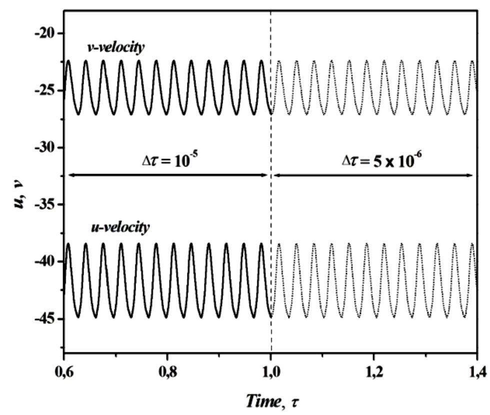

(b)

Fig. 3. Temporal evolutions of the dimensionless axial velocity component v, radial velocity component u, and temperature θ at monitoring point S_8 at φ = 45°, (a) steady state for Gr = 8×10^5, (b) Comparison of the results between two time steps for Gr_{cr}= 9×10^5 and Ha = 0.

To detect the critical Grashof number Gr_{cr} of bifurcation from steady (Fig. 3a) to unsteady flows, we carry out a succession of numerical calculations, by increasing the Grashof number in predetermined intervals. The instabilities found for a dimensionless time increment $\Delta\tau$ can be numerical (no physical); then to eliminate these numerical instabilities, we recomputed the solution obtained with the same flow parameters, but with a new time increment $\Delta\tau/2$ (Ghernaout *et al*. 2014). If the amplitudes of oscillations remain the same ones in all the monitoring points after reduction of the time increment this instability will be physical (Fig. 3b).

Figures 4a-b, show the time evolution of the dimensionless temperature θ and radial velocity u, respectively at different monitoring points for $Gr_{cr} = 9\times10^5$ and $\varphi = 45°$. The flow oscillates in a simple periodic manner around the averaged values. Each points of the fluid domain chosen in this investigation are characterized by a particular signal (shape, amplitude, frequency or other characteristics). We note that the temporal resolution effects are investigated by using successive time steps until no differences are observed in the amplitude of oscillations. As expected, the amplitude of the dimensionless temperature θ is smallest compared to the dimensionless radial velocity u.

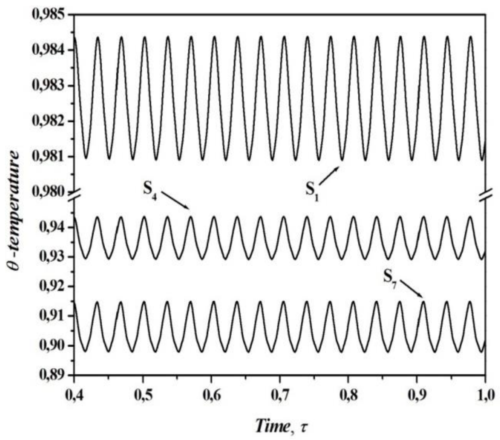

(a)

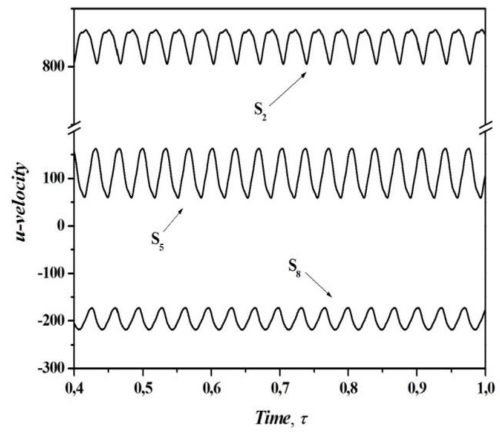

(**b**)

Fig. 4. Time evolution of the dimensionless temperature θ at S_1, S_4 and S_7 (a), and dimensionless radial velocity component u at S_2, S_5 and S_8 (b), for $Gr_{cr} = 9\times10^5$, $\varphi = 45°$and Ha = 0.

In order to obtain the energy spectrum of oscillations, we have used the fast Fourier transform (FFT) of a number N_{ech} of samples of the time variations of various dimensionless parameters. This transform, once multiplied by the half of its conjugate quantity, gives the power spectrum density (PSD) as a function of the oscillation frequencies (Fig. 5), defined by: $F = k / (N_{ech}\times\Delta\tau)$, where $\Delta\tau$ is the dimensionless time step and k = 1, 2, N_{ech} / 2. Energy has been normalized by N^2_{ech}. The dimensionless predominant frequencies are considered as those playing the main role in the flow oscillation there can exist several others frequencies which are multiples of the dominant one (Stevens *et al*. 1999).

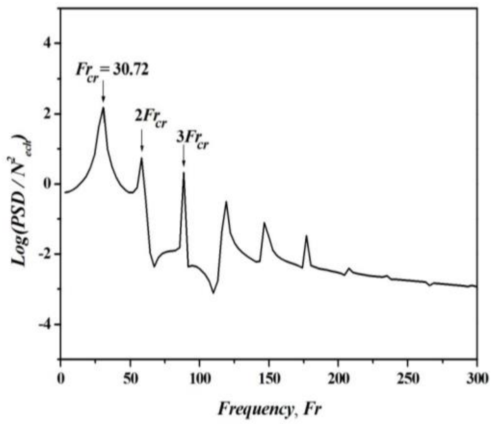

Fig. 5. Power spectrum of the dimensionless radial velocity component u, for $Gr_{cr} = 9\times10^5$, $\varphi = 45°$ and Ha = 0. $Fr_{cr} = 30.72$, represent the dimensionless critical frequency.

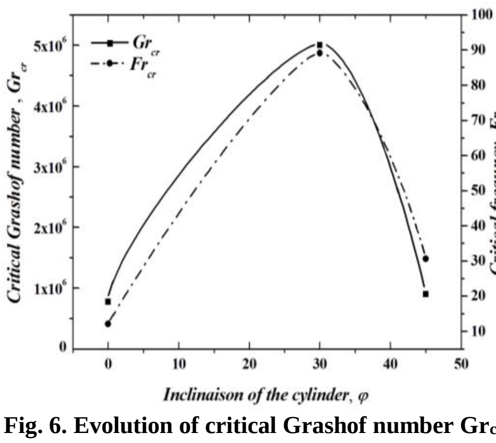

Fig. 6. Evolution of critical Grashof number Gr_{cr} and corresponding frequency Fr_{cr} for different inclinations of the enclosure.

The effect of the inclinations of the cylinder on the flow stability is shown in Fig. 6, which displays the evolution of the critical Grashof number Gr_{cr} and corresponding frequency Fr_{cr} for different inclinations of the cylinder φ. It can be seen that the variation of the angle of inclination of the cylinder to a significant effect on the stabilization of the flow and that the stabilization is better for the angle of inclination $\varphi = 30°$ corresponding to a number of critical Grashof $Gr_{cr}= 4.1\times10^6$.

4.3 Effect of Magnetic Field Orientation on the Oscillatory Natural Convection (Ha ≠ 0)

In this section, we are interested in the oscillatory solution of the flow convection with different orientations of magnetic field ($\delta = 0°$, 30°, 45° and 90°). For this goal, we fixed the cylinder without inclination ($\varphi = 0°$). According to the work of Bouabdallah *et al*. (2011), we report only the results for positive angles, and note that for negative angles ($-\delta$), the same results are obtained in the range $0 \leq \delta \leq 90°$.

In general, the magnetic field suppresses the fluid motion and reduces the heat transfer rate. As the Hartmann number increases, the temperature gradients become less abrupt and the convection effect become less intense, resulting in smaller velocities. Thus, the increase of the magnetic field favors the conduction heat transfer. Our numerical simulations are presented for various values of the Hartmann number.

To see the effect of magnetic field on the oscillatory flow regime, we applied the magnetic field in radial direction ($\delta = 0°$). The Fig. 7, present the time-dependent of the axial velocity component in one period, for Grashof number $Gr = 2.1\times10^6$ at angle of inclination of the cylinder equal $\varphi = 0°$, and for various Hartmann numbers (Ha = 10, 20, 30, 40 and 50). It is clearly that the increase of Hartmann number (intensity of magnetic field), stabilize the oscillatory flow and reduce the magnitude of velocity (Raja *et al*. 2013). The flow regime is oscillatory for Ha = 10, and stabilized to steady state flow when Ha > 10. This is translates the ability of the magnetic field on the stability of convective flows, this reduction due to radial Lorentz force which slows the velocity of particles.

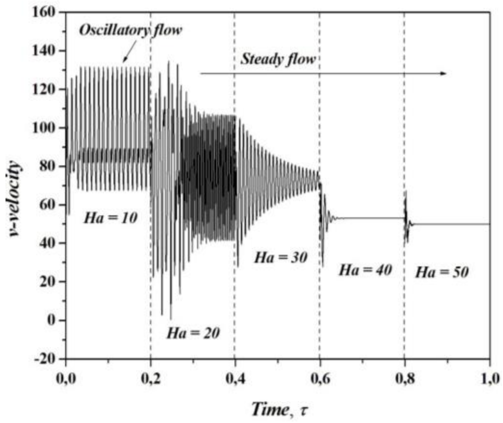

Fig. 7. Effect of magnetic field on the time dependent v-velocity component at monitoring point S_7, for $Gr = 2.1\times10^6$ and $\delta = 0°$, for different Hartmann number ($\varphi = 0°$ and $Ha \leq 50$).

In order to explain the nature of the flow oscillatory, we connect the temporal evolution of the dimensionless axial velocity v at point S_8 during one period with evolution of the flow structure (streamline and temperature field) at various dimensionless times: τ_a, τ_b, τ_c, τ_d, τ_e and τ_f, for $Gr_{cr} = 9\times10^6$, $\varphi = 0°$, $\delta = 0°$ and Ha = 30 (Fig. 8). The flow field presents two cells. These cells dilate and narrow during the time (τ_a, τ_b, τ_c, τ_d, τ_e and τ_f). At time τ_a, the structure characterized by a small cell located in bottom of liquid and separated by another secondary recirculation cell (dashed lines) in top of enclosure with a negative mass flow. At times τ_b, τ_c, τ_d and τ_e the size of secondary recirculation cell change and narrowing gradually in the axial direction, after (at time τ_f) this cell dilate gradually. We note that, the streamlines structure at the time τ_a is identical at the time τ_f, which means that the oscillatory flow is periodic. The temperature field is very significant in this case where the magnetic field is applied in radial direction ($\delta = 0°$), and shows the existence and the predominance of the convective mode compared to the diffusive mode (deformation of the isotherms).

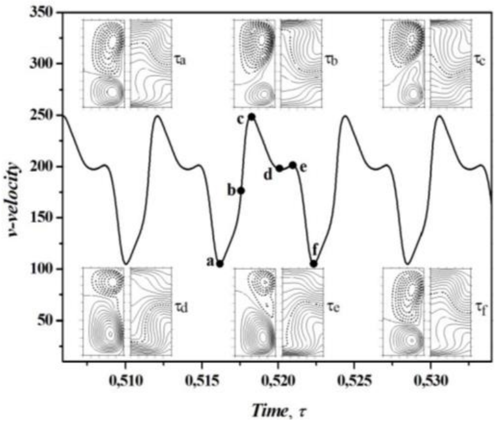

Fig. 8. Time evolution of the dimensionless axial velocity v in oscillatory flow at point S_8, with streamlines and isotherms at various dimensionless time: τ_a, τ_b, τ_c, τ_d, τ_e and τ_f, for $Gr_{cr} = 9\times10^6$ and $\varphi = 0°$. The magnetic field is applied in the radial direction ($\delta = 0°$ and Ha = 30).

Figures 9a-b, show the magnetohydrodynamic stability diagram (Gr_{cr} – Ha) and (Fr_{cr} –Ha) for different orientation of magnetic field ($\delta = 0°$, 30°, 45° and 90°). No tilting in the cylinder enclosure ($\varphi = 0°$). We can see that the strong dependence between the onset of oscillatory flow (the critical Grashof number and corresponding frequency) and the orientation of magnetic field, where the strongest damping of the flow is obtained when the magnetic field is applied along the radial direction ($\delta = 0°$). These results are in good agreement with those obtained by Oudina and Bessaïh (2014) and Sankar *et al*. (2006). They found a better stabilization of the flow where the magnetic field applied in the radial direction.

To give the combination between the inclinations of the enclosure and the magnetic field orientation on oscillatory flow, we have presented the evolution of critical Grashof number and frequency for different Hartmann number associated with different orientation of magnetic field for inclination of the cylinder equal to φ = 30° and φ = 45°, respectively (Figs. 10a-b and Figs. 11a-b). In these figures we are presented the value of critical Grashof number corresponds of the best stabilization by tilting the cylinder (φ = 30°, without magnetic field) by a dotted line for comparison with the results.

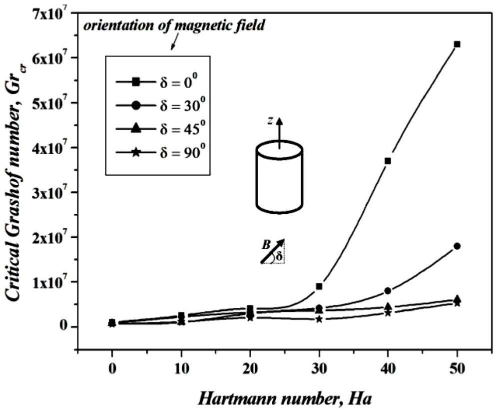

(a)

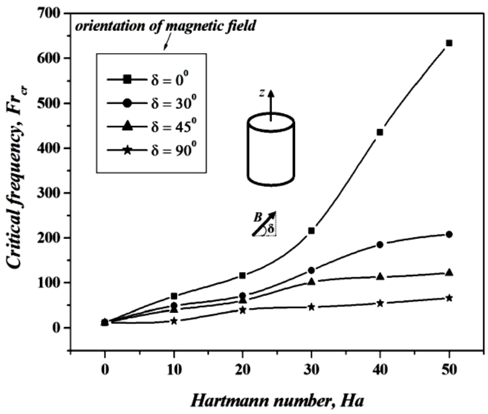

(b)

Fig. 9. Magnetohydrodynamic stability diagram for different orientation of magnetic field (a) Gr_{cr} – Ha and (b) Fr_{cr} – Ha. No tilting in the enclosure (φ = 0° and Ha ≤ 50).

4.4 Combination between the Inclinations of the Enclosure and Magnetic Field (Ha ≠ 0 and φ ≠ 0)

There has been a significant increase in Grashof number during the increase of the intensity of magnetic field and similarly for the corresponding frequency, and can always see the best stabilization found for inclination of the cylinder φ = 30° and the radial direction of the magnetic field (δ = 0°). Also we can find from these figures that can stabilize the convective flow by different methods according to the available possibilities. Either, by a tilting of the cylinder enclosure (if we haven't the possibilities to apply a magnetic field), or applied of magnetic field in fairly orientation, or by the combination of both for a better stabilization. For example, if we take (from Fig. 10a and Fig. 11a) the number of critical value of $Gr = 4.1 \times 10^6$, we can reach that number by:

- Inclination of the cylinder by φ = 30° without magnetic field (Ha = 0).
- Inclination of the cylinder by φ = 45° and applied of magnetic field with orientation δ = 45° (Ha = 20).
- Inclination of the cylinder by φ = 45° and applied of magnetic field in transverse direction, δ = 90° (Ha = 30).

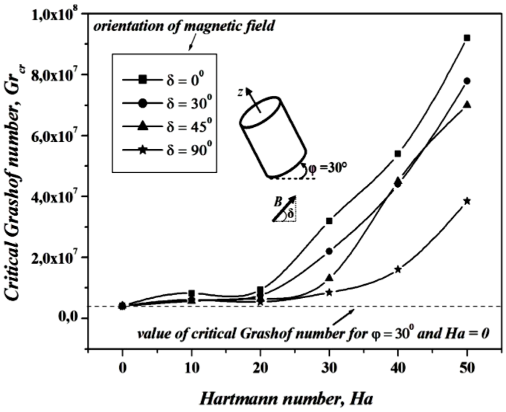

(a)

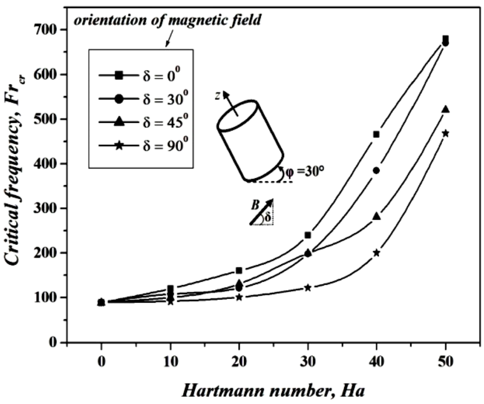

(b)

Fig. 10. Magnetohydrodynamic stability diagram for different orientations of magnetic field, (a) Gr_{cr} – Ha and (b) Fr_{cr} – Ha. The enclosure has a fixed inclination φ = 30° (Ha ≤ 50).

Figure 12, shows a comparison between the case where the angle of inclination of the cylinder and magnetic field orientation are the same (φ = δ), it is clear that the best stabilization is found where the inclination of cylinder and magnetic field orientation equal an φ = δ = 30°.

5. CONCLUSION

The combination between the inclinations of the enclosure and the effect of magnetic field orientation on the oscillatory natural convection has been numerically studied. The study was carried out in the oscillatory state, for different cases: inclination of the cylinder (φ = 0°,30° and 45°), under the effect of magnetic field in different orientations ($\delta = 0$, 30°, 45° and 90°, $Ha \leq 50$) and the combination between them.

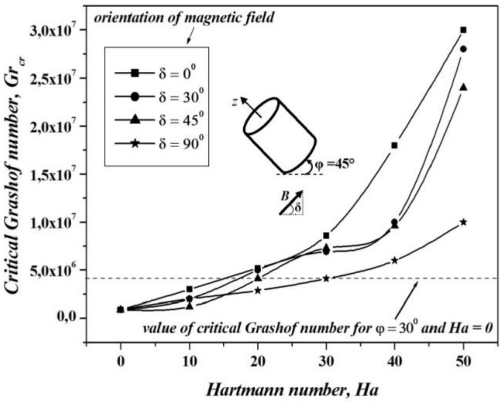

(a)

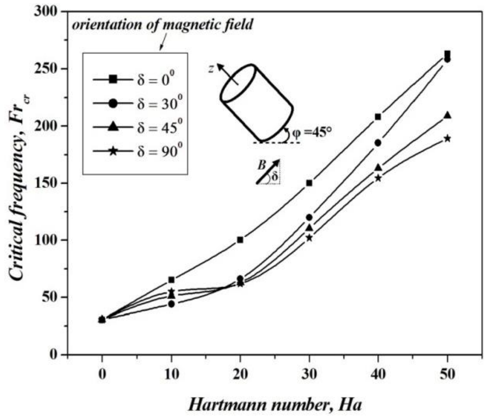

(b)

Fig. 11. Magnetohydrodynamic stability diagram for different orientation of magnetic field, (a) Gr_{cr} – Ha and (b) Fr_{cr} – Ha. The enclosure has a fixed inclination φ = 45° ($Ha \leq 50$).

The obtained results have been compared with the available data (experimental/ numerical) from the literature and good agreement has been found. The main results are as follows:

- The variation of inclination of the cylinder has a significant effect on the stabilization of the flow, and shows that the best stabilization of oscillatory natural convection is obtained at the inclination of the cylinder by φ = 30°, where the corresponding critical Grashof number equal $Gr_{cr} = 4.1\times10^6$.
- A strong dependence between the direction of the magnetic field and the critical Grashof number and their corresponding frequency as summarized in the magnetohydrodynamic stability diagram.
- A radial magnetic field ($\delta = 0°$), provides a strong stabilization of the flow field, where the high value of critical Grashof number is obtained for this case.
- The combination between the inclinations of the cylinder enclosure and the orientation of magnetic field has also a significant effect on the stabilization of the flow, and that the best stabilization is found for two cases: the case of inclined enclosure at φ = 30° and the applied of radial magnetic field ($\delta = 0°$), and the case of the same inclination of the enclosure and magnetic field $\varphi = \delta = 30°$.

The obtained results in this study may allow researchers and industrialists to know the oscillatory modes of conducting fluid in an inclined cylindrical enclose with and without magnetic field, and help them for the stabilization according to the available possibilities, in order to improve the quality of the semiconductors obtained during the crystal growth.

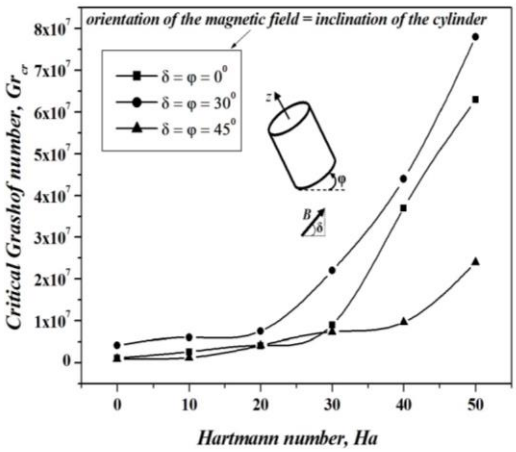

Fig. 12. Magnetohydrodynamic stability diagram in both combined case: inclination of the cylinder enclosure and orientation of the magnetic field (φ = δ), for different Hartmann number.

REFERENCES

Alchaar, S., P. Vasseur and E. Bilgen (1995). The effect of a magnetic field on natural convection in a shallow cavity heated from below. *Chemical Engineering Communications* 134(1), 195–209.

Al-Najem, N. M., K. M. Khanafer and M. M. El-Refaee (1998). Numerical Study of laminar natural convection in tilted enclosure with transverse magnetic field. *International Journal of Numerical Methods for Heat and Fluid Flow* 8(6), 651–672.

Atia, A., S. Bouabdallah, M. Teggar and A. Benchatti (2015). Numerical study of mixed convection in cylindrical Czochralski configuration for crystal growth of silicon. *International Journal of Heat and Technology* 33(1), 39–46.

Battira, M. and R. Bessaïh (2008). Three-dimensional natural convection in the horizontal Bridgman configuration under various wall electrical conductivity and magnetic field. *Numerical Heat Transfer* 55(1), 58–76.

Bessaïh, R. and S. Bouabdallah (2008). Numerical study of oscillatory natural convection during solidification of a liquid metal in a rectangular enclosure with and without magnetic field. *Numerical Heat Transfer* 54(3), 331–348.

Bessaïh, R., A. Boukhari and P. Marty (2009). Magnetohydrodynamics stability of a rotating flow with heat transfer. *International Communications in Heat and Mass Transfer* 36(9), 893–901.

Bontoux, P., C. Smutek, A. Randriamampianina, B. Roux, G. P. Extrémet, A. C. Hurford, F. Rosenberger and G. De Vahl Davis (1986). Numerical solutions and experimental results for three-dimensional buoyancy driven flows in tilted cylinders. *Advances in Space Research* 6(5), 155–160.

Bouabdallah, S. and R. Bessaïh (2012). Effect of magnetic field on 3D flow and heat transfer during solidification from a melt. *International Journal of Heat and Fluid Flow* 37, 154–166.

Bouabdallah, S., R. Bessaïh, B. Ghernaout and A. Benchatti (2011). Effect of an external magnetic field on 3-D oscillatory natural convection of molten gallium during phase change. *Numerical Heat Transfer* 60(1), 84–105.

Bühler, L. (1995). Magnetohydrodynamic flows in arbitrary geometries in strong, non-uniform magnetic fields: A numerical code for the design of fusion reactor blankets. *Fusion Science and Technology* 27(1), 3–24.

Cerisier, P. and S. Rahal (1996). Experimental study of the competition between convective rolls in an enclosure. *Dynamics of Multiphase Flows across Interfaces* 467, 105–116.

Cessi, P. and W. R. Young (1992). Fixed-flux convection in a tilted slot. *Journal of Fluid Mechanics* 237, 57–71.

Delgado-Buscalioni, R. and E. Crespo del Arco (2001). Flow and heat transfer regimes in inclined differentially heated cavities. *International Journal of Heat and Mass Transfer* 44(10), 1947–1962.

Garandet, J. P., T. Alboussiere and R. Moreau (1992). Buoyancy-driven convection in a rectangular enclosure with a transverse magnetic field. *International Journal of Heat and Mass Transfer* 35(4), 741–748.

Gelfgat, A. Y. and P. Z. Bar-Yoseph (2001). The effect of an external magnetic field on oscillatory instability of convective flows in a rectangular cavity. *Physics of Fluids* 13(8), 2269–2279.

Gelfgat, A. Y. and I. Tanasawa (1994). Numerical analysis of oscillatory instability of buoyancy convection with the Galerkin spectral method. *Numerical Heat Transfer* 25(6), 627–648.

Ghernaout, B., S. Bouabdallah, A. Benchatti and R. Bessaïh (2014). Effect of the buoyancy ratio on oscillatory double-diffusive convection in binary mixture. *Numerical Heat Transfer* 66(8), 928–946.

Ghosh, S. K. (1991). A note on steady and unsteady hydromagnetic flow in a rotating channel in the presence of inclined magnetic field. *International Journal of Engineering Science* 29(8), 1013–1016.

Ghosh, S. K. (1997). A note on unsteady hydromagnetic flow in a rotating channel permeated by an inclined magnetic field in the presence of an oscillator. *Czechoslovak Journal of Physics* 47(8), 787–792.

Ghosh, S. K., O. A. Bég, J. Zueco and V. R. Prasad (2010). Transient hydromagnetic flow in a rotating channel permeated by an inclined magnetic field with magnetic induction and maxwell displacement current effects. *Zeitschrift für angewandte Mathematik und Physik* 61(1), 147–169.

Ghosh, S. K. and I. Pop (2002). A note on a hydromagnetic flow in a slowly rotating system in the presence of an inclined magnetic field. *Magnetohydrodynamics* 38(4), 377–384.

Kakarantzas, S. C., I. E. Sarris, A. P. Grecos and N. S. Vlachos (2009). Magnetohydrodynamic natural convection in a vertical cylindrical cavity with sinusoidal upper wall temperature. *International Journal of Heat and Mass Transfer* 52(1-2), 250–259.

Karcher, C., Y. Kolesnikov, O. Andreev and A. Thess (2002). Natural convection in a liquid metal heated from above and influenced by a magnetic field. *European Journal of Mechanics- B/ Fluids* 21(1), 75–90.

Lock, G. S. H. and J. Fu (1993). Natural convection in the inclined cranked thermosyphon. *Journal of Heat Transfer* 115(1), 167–172.

Mahfoud, B. and R. Bessaïh (2012). Stability of swirling flows with heat transfer in a cylindrical enclosure with CO/Counter-rotating end disks under an axial magnetic field. *Numerical Heat Transfer* 61(6), 463–482.

Markham, B. L. and F. Rosenberger (1984). Diffusive-convective vapor transport across horizontal and inclined rectangular enclosures. *Journal of Crystal Growth* 67(2), 241–254.

Oreper, G. M. and J. Szekely (1983). The effect of an externally imposed magnetic field on buoyancy driven flow in a rectangular cavity. *Journal of Crystal Growth* 64(3), 505–515.

Oudina, F. M. and R. Bessaïh (2014). Numerical modeling of MHD stability in a cylindrical configuration. *Journal of the Franklin Institute* 351(2), 667–681.

Ozoe, H. and M. Maruo (1987). Magnetic and gravitational natural convection of melted silicon two dimensional numerical computations for the rate of heat transfer. *JSME* 30(263), 774–784.

Patankar, S. V. (1980). *Numerical Heat Transfer and Fluid Flow*, McGraw-Hill, New-York.

Piazza, I. D. and M. Ciofalo (2002). MHD free convection in a liquid-metal filled cubic enclosure. II. Internal heating. *International Journal of Heat and Mass Transfer* 45(7), 1493–1511.

Raja, T., S. Karthikeyan and B. Senthilnathan (2013). A magneto-convection over a semi-infinite porous plate with heat generation. *Journal of Applied Fluid Mechanics* 6(4), 589–595.

Ramana Reddy, G. V., N. Bhaskar Reddy and A. J. Chamkha (2016). MHD mixed convection oscillatory flow over a vertical surface in a porous medium with chemical reaction and thermal radiation. *Journal of Applied Fluid Mechanics* 9(3), 1221–1229.

Rudraiah, N., R. M. Barron, M. Venkatachalappa and C. K. Subbaraya (1995). Effect of a magnetic field on free convection in a rectangular enclosure. *International Journal of Engineering Science* 33(8), 1075–1084.

Sankar, M., M. Venkatachalappa and I. S. Shivakumara (2006). Effect of magnetic field on natural convection in a vertical cylindrical annulus. *International Journal of Engineering Science* 44(20), 1556–1570.

Seth, G. S. and S. K. Ghosh (1986). Unsteady hydromagnetic flow in a rotating channel in the presence of inclined magnetic Field. *International Journal of Engineering Science* 24(7), 1183–1193.

Seth, G. S., R. Nandkeolyar and Md. S. Ansari (2012). Effects of hall current and rotation on unsteady MHD couette flow in the presence of an inclined magnetic field. *Journal of Applied Fluid Mechanics* 5(2), 67–74.

Stevens, J. L., J. M. Lopez and B. J. Cantwell (1999). Oscillatory flow states in an enclosed cylinder with a rotating end wall. *Journal of Fluid Mechanics* 389, 101–118.

Tagawa, T. and H. Ozoe (1997). Enhancement of heat transfer rate by application of a static magnetic field during natural convection of a liquid metal in a cube. *Journal of Heat Transfer* 119(2), 265–271.

Tagawa, T. and H. Ozoe (1998). Enhanced heat transfer rate measured for natural convection in liquid gallium in a cubical enclosure under a static magnetic field. *Journal of Heat Transfer* 120(4), 1027–1032.

Viskanta, R., D. M. Kim and C. Gau (1986). Three-dimensional natural convection heat transfer of a liquid metal in a cavity. *International Journal of Heat and Mass Transfer* 29(3), 475–485.

Wirtz, R. A. and W. F. Tsheng (1970). Finite difference simulation of free convection in tilted enclosures of low aspect ratio. In *Numerical Methods in Thermal Problems I*, Pineridge, UK, Swansea 242, 381–390.

Wirtz, R. A. and W. F. Tsheng (1980). Natural Convection across Tilted Rectangular Enclosures of Small Aspect Ratio. In J. Catton and K. E. Torrance (Eds.) *Natural convection in enclosures*, ASME 8, 54–67.

Woods, A. W. and S. J. Linz (1992). Natural convection and dispersion in inclined fracture. *Journal of Fluid Mechanics* 241, 59–74.